DOI: 10.6060/ivkkt.20266902.7272

УДК: 547.724

СИНТЕЗ, МОЛЕКУЛЯРНЫЙ ДОКИНГ И ИЗУЧЕНИЕ *in-vitro* АНТИМИКРОБНОЙ АКТИВНОСТИ ИМИНОДИГИДРОФУРАНОВ, СОДЕРЖАЩИХ 4-ТИАЗОЛИДИНОНОВОЕ КОЛЬЦО

Г.Г. Токмаджян, Л.В. Карапетян, А.Г. Сукиасян, С.Г. Чайлян, Р. Капаварапу, Р.А. Мадоян

Гаяне Геворковна Токмаджян (ORCID 0000-0002-2561-8494), Лусине Владимировна Карапетян (ORCID 0000-0002-9765-6131)*

Кафедра органической химии факультета химии, Ереванский государственный университет, ул. Алекса Манукяна, 1, Ереван, 0025, Армения
E-mail: lkarapetyan@ysu.am*

Анна Григорьевна Сукиасян, Самвел Григорьевич Чайлян, Роза Александровна Мадоян

Лаборатория аналитической хроматографии, Институт биохимии им. Г. Буниатяна НАН РА, ул. Паруйра Севаки, 5/1, Ереван, 0014, Армения

Равикумар Капаварапу

Кафедра фармацевтической химии и фитохимии, Нирмала Фармацевтический колледж, Мангалагири-522503, Андхра-Прадеш, Индия

Инфекции, вызываемые микробами, являются основной причиной смерти во всем мире. Растущая устойчивость различных патогенных бактерий, включая E. coli, S. aureus и грибы Candida, к антибиотикам и противогрибковым препаратам стала в последние годы серьезной проблемой общественного здравоохранения. Ограниченное количество антибиотиков для лечения инфекций и постоянное развитие устойчивости к используемым антимикробным и противогрибковым препаратам представляют собой серьезную проблему. Открытие новых, безопасных и высокоэффективных антибактериальных и противогрибковых соединений против патогенов является очень актуальной задачей. 2-Имино-2,5-дигидрофураны являются N-содержащими аналогами O-содержащих биологически активных соединений. Учитывая высокую биологическую активность производных 2-оксо-2,5-дигидрофурана и 4-тиазолидинона, были изучены in silico и in vitro антибактериальные и противогрибковые свойства синтетических соединений, содержащих иминодигидрофурановые и 4-тиазолидиноновые кольца. Мы синтезировали соединения этил-2-(4-оксо-2-((4-метил-5,5-диалкил-3-(алкил(арил, бензил, циклоалкил)карбамоил)фуран-2(5H)-илиден)гидразоно)тиазолидин-5-илиден)ацетат 3a-3i и 2-(4-оксо-2-((4-метил-5,5-диалкил-3-(алкил(арил, бензил, циклоалкил)карбамоил)фуран-2(5H)-илиден)гидразоно)тиазолидин-5-ил)уксусная кислота 5a-5i, содержащие иминодигидрофурановые и тиазолидиноновые кольца, путем последующей реакции присоединения Михаэля/гетероциклизации из иминодигидрофурановых тиосемикарбазонов. Соединения 2-(4-оксо-2-((4,5,5-триметил-3-карбамоил)фуран-2(5H)-илиден)гидразоно)тиазолидин-5-ил)уксусная кислота (5a), 2-(4-оксо-2-((4,5,5-триметил-3-фенилкарбамоил)фуран-2(5H)-илиден)гидразоно)тиазолидин-5-ил)уксусная кислота (5d), 2-(4-оксо-2-((4,5,5-триметил-3-бензилкарбамоил)фуран-2(5H)-илиден)гидразоно)тиазолидин-5-ил)уксусная кислота (5g), 2-(4-оксо-2-((4-метил-5,5-пентаметилен-3-бензилкарбамоил)фуран-2(5H)-илиден)гидразоно)тиазолидин-5-ил)уксусная кислота (5h) обладают выраженной антимикробной активностью против 3 патогенных микроорганизмов. Результаты показали, что тестируемые организмы испытали заметное ингибирование роста грибков и бактерий. Профили ADMET показали, что эти соединения, особенно 2-(4-оксо-2-((4-метил-5,5-пентаметилен-3-бензилкарбамоил)фуран-2(5H)-илиден)гидразоно)тиазолидин-5-ил)уксусная кислота (5h), с самой высокой абсорбцией в кишечнике человека, обладают благоприятными характеристиками для дальнейшей оптимизации и разработки. Хотя они проявляют гепатотоксичность, уточнение их фармакокинетических свойств имеет важное значение для продвижения этих соединений в качестве потенциальных противомикробных агентов.

Ключевые слова: антибактериальная и противогрибковая активность, иминодигидрофуран, 4-тиазолидинон, молекулярный докинг

SYNTHESIS, MOLECULAR DOCKING AND *in-vitro* ANTIMICROBIAL ACTIVITY STUDY OF IMINODIHYDROFURANS CONTAINING 4-THIAZOLIDINONE RING

G.G. Tokmajyan, L.V. Karapetyan, A.G. Sukiasyan, S.G. Chailyan, R. Kapavarapu, R.A. Madoyan

Gayane G. Tokmajyan (ORCID 0000-0002-2561-8494), Lusine V. Karapetyan (ORCID 0000-0002-9765-6131)*

Department of Organic Chemistry, Faculty of Chemistry, Yerevan State University, Alex Manoogian ave., 1, Yerevan, 0025, Armenia
E-mail: lkarapetyan@ysu.am*

Anna G. Sukiasyan, Samvel G. Chailyan, Roza A. Madoyan

Laboratory of Analytical Chromatography, Institute of Biochemistry named after H. Buniatyan, NAS RA, Paruyr Sevaki st., 5/1, Yerevan, 0014, Armenia

Ravikumar Kapavarapu,

Department of Pharmaceutical Chemistry and Phytochemistry, Nirmala College of Pharmacy, Mangalagiri-522503, Andhra Pradesh, India

Infections caused by microbes are a major cause of death worldwide. The increasing resistance of various pathogenic bacteria, including E. coli, S. aureus and Candida fungi, to antibiotics and antifungals has become a major public health problem in recent years. The limited number of antibiotics for the treatment of infections and the continuous development of resistance to the used antimicrobial and antifungal drugs pose a serious challenge. The discovery of new, safe and highly effective antibacterial and antifungal compounds against pathogens is very urgent. 2-Imino-2,5-dihydrofurans are N-containing analogs of O-containing biologically active compounds. Considering the enormous biological potential of 2-oxo-2,5-dihydrofuran and 4-thiazolidinone derivatives, synthetic compounds containing iminodihydrofuran and 4-thiazolidinone rings were studed for antibacterial and antifungal activities in silico and in vitro. We synthesized compounds ethyl 2-(4-oxo-2-((4-methyl-5,5-dialkyl-3-(alkyl(aryl, benzyl, cycloalkyl)carbamoyl)furan-2(5H)-ylidene)hydrazono)thiazolidin-5-ylidene)acetate 3a-3i and 2-(4-oxo-2-((4-methyl-5,5-dialkyl-3-(alkyl(aryl, benzyl, cycloalkyl)carbamoyl)furan-2(5H)-ylidene)-hydrazono)thiazolidin-5-yl)acetic acid 5a-5i comprising iminodihydofuran and thiazolidinone rings by subsequent Michael addition/heterocyclization reaction from iminodihydrofuran thiosemicarbazones. Compounds 2-(4-oxo-2-((4,5,5-trimethyl-3-carbamoyl)furan-2(5H)-ylidene)hydrazono)thiazolidin-5-yl)acetic acid (5a), 2-(4-oxo-2-((4,5,5-trimethyl-3-phenylcarbamoyl)furan-2(5H)-ylidene)hydrazono)thiazolidin-5-yl)acetic acid (5d), 2-(4-oxo-2-((4,5,5-trimethyl-3-benzylcarbamoyl)furan-2(5H)-ylidene)hydrazono)thiazolidin-5-yl)acetic acid (5g), 2-(4-oxo-2-((4-methyl-5,5-penthamethylene-3-benzylcarbamoyl)furan-2(5H)-ylidene)hydrazono)thiazolidin-5-yl)acetic acid (5h) have pronounced antimicrobial activity against 3 pathogenic microorganisms. The results indicated that the tested organisms experienced a noticeable inhibition of fungal and bacterial growth. The ADMET profiles indicate that these compounds, particularly 2-(4-oxo-2-((4-methyl-5,5-penthamethylene-3-benzylcarbamoyl)furan-2(5H)-ylidene)hydrazono)thiazolidin-5-yl)acetic acid (5h) with the highest human intestinal absorption, possess favorable characteristics for further optimization and development. Although they exhibit hepatotoxicity, refining their pharmacokinetic properties is essential for advancing these hit compounds as potential antimicrobial agents.

Keywords: antibacterial and antifunfal activity, iminodihydrofuran, 4-thiazolidinone, molecular docking

Для цитирования:
Токмаджян Г.Г., Карапетян Л.В., Сукиасян А.Г., Чайлян С.Г., Капаварапу Р., Мадоян Р.А. Синтез, молекулярный докинг и изучение *in-vitro* антимикробной активности иминодигидрофуранов, содержащих 4-тиазолидиноновое кольцо. *Изв. вузов. Химия и хим. технология*. 2026. Т. 69. Вып. 2. С. 78–91. DOI: 10.6060/ivkkt.20266902.7272.

For citation:
Tokmajyan G.G., Karapetyan L.V., Sukiasyan A.G., Chailyan S.G., Kapavarapu R., Madoyan R.A. Synthesis, molecular docking and *in-vitro* antimicrobial activity study of iminodihydrofurans containing 4-thiazolidinone ring. *ChemChemTech* [*Izv. Vyssh. Uchebn. Zaved. Khim. Khim. Tekhnol*.]. 2026. V. 69. N 2. P. 78–91. DOI: 10.6060/ivkkt.20266902.7272.

INTRODUCTION

Research in the field of synthesis of biologically active compounds is one of the promising areas in organic chemistry [1-3]. Infections caused by microbes are a major cause of death worldwide. The increasing resistance of various pathogenic bacteria, including *E. coli*, *S. aureus* and *Candida* fungi, to antibiotics and antifungals has become a major public health problem in recent years. The limited number of antibiotics for the treatment of infections and the continuous development of resistance to the used antimicrobial and antifungal drugs pose a serious challenge [4]. The discovery of new, safe and highly effective antibacterial and antifungal compounds against pathogens is very urgent and hence the only way to address the problem of resistance and develop successful treatments for infectious diseases [5-7].

Several 4-thiazolidinone based drugs such as ralitoline (anticonvulsant), ethozolin (loop diuretic) and pioglitazone (oral anti-diabetic drug) are already approved for therapeutic use. The 4-thiazolidinone ring has other important biological effects such as anti-inflammatory, antioxidant, platelet-activating factor (PAF) antagonist, cyclooxygenase (COX) inhibition, tumor necrosis factor antagonist, as well as anticancer, anticonvulsant, antimicrobial, antiviral and anti HIV effects [8-13].

2-Imino-2,5-dihydrofurans are *N*-containing analogs of O-containing biologically active compounds, 2-oxo-2,5-dihydrofurans, which are found in many natural and synthetic compounds. The 2-oxo-2,5-dihydrofuran scaffolds represent important therapeutic classes with a wide range of biological activities [14-20]. The 2-imino-2,5-dihydrofuran derivatives often exhibit equally valuable properties [21-24]. Considering the enormous biological potential of 2-oxo-2,5-dihydrofuran and 4-thiazolidinone derivatives, synthetic compounds containing iminodihydrofuran and 4-thiazolidinone rings [25, 26] were chosen to study the antibacterial and antifungal activities *in silico* and *in vitro*.

RESULTS AND DISCUSSION

A convenient synthetic route to the 4-thiazolidinone ring involving a Michael addition/heterorocyclization sequence was developed (Scheme 1). Reactions of iminodihydrofuran thiosemicarbazones **1a-1i** [27, 28] with diethylacetylene dicarboxylate **2** were carried out in absolute ethanol at room temperature for 10-12 h, which leads to iminodihydrofuran derivatives containing a thiazolidinone ring, in particular, ethyl 2-(4-oxo-2-((4-methyl-5,5-dialkyl-3-(alkyl(aryl, benzyl, cycloalkyl)carbamoyl)furan-2(5H)-ylidene)hydrazono)thiazolidin-5-ylidene)acetate **3a-3i** in high yields (86-91%). Reactions of iminodihydrofuran thiosemicarbazones **1a-1i** with maleic anhydride **4** were carried out in absolute ethanol or chloroform under reflux for 10-15 h, yielding iminodihydrofuran derivatives, containing thiazolidinone ring, in particular 2-(4-oxo-2-((4-methyl-5,5-dialkyl-3-(alkyl(aryl, benzyl,cycloalkyl)carbamoyl)furan-2(5H)-ylidene)hydrazono)thiazolidin-5-yl)acetic acid **5a-5i** with good (76-83%) yields [25, 26].

All synthesized compounds **3a-3i** and **5a-5i** (Scheme 1) [25, 26] were tested for antibacterial activity against Gram-positive (S. aureus) and Gram-negative (*E. coli*) bacteria and antifungal activity against the fungus (*C. albicans*) by agar diffusion method [29]. Furadonin, Furazolidone and Fluconazole were used as standards for comparison of antibacterial and antifungal activity [30]. DMSO showed no zones of inhibition.

Compounds **5a, 5d, 5g, 5h** have pronounced antimicrobial activity against 3 pathogenic microorganisms. Compounds **5a, 5g, 5h** showed higher antibacterial activity against the bacteria *S. aureus* and *E. coli* than the standard drugs Furadonin and Furazolidone. Compounds **5g, 5h** showed antifungal activity against the fungus *C. albicans*. Despite fluconazole used as a reference drug against *C. albicans*, it doesn't have antibacterial properties against *E. coli* and S. *aureus*. Unlike fluconazole, the new synthesized compounds also have superior antibacterial properties against *E. coli* (30 mm) and *S. aureus* (30 mm).

Comparative analyses were conducted to compare the antifungal activity of the obtained compounds with Fluconazole. Different concentrations (50 mg/ml and 150 mg/ml) of fluconazole were used. The zones of inhibition of *C. albicans* growth under the influence of Fluconazole were 25 mm and 33 mm, respectively. However, the zones were not clean and seeded with fungal cells. There are some Candida fungal cells that are resistant to fluconazole. Analyses of the results showed that the tested compounds had better activity against bacterial strains in comparison to the fungal strain.

The structure-activity relationship (SAR) suggested that the potency of compounds **5a, 5g** and **5h**

could be attributed to the presence of the carboxamide and *N*-benzylcarboxamide substituents in the 3-position and dimethyl, pentamethylene substituents in the 5-position of the dihydrofuran ring, which is accounted for their significant antibacterial activity.

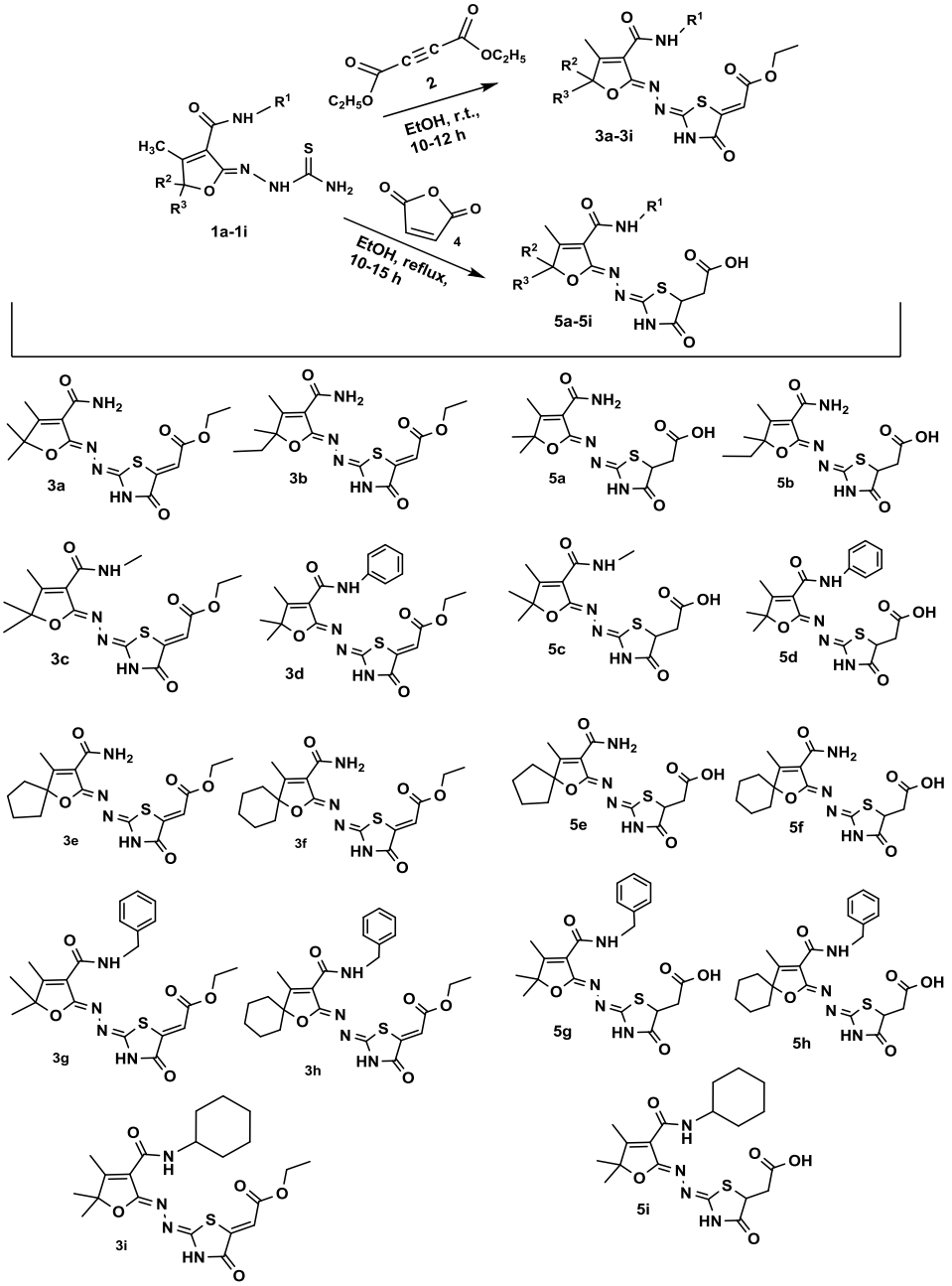

Scheme. Catalyst-free synthesis of compounds **3a–3i** and **5a–5i**
Схема. Синтез соединений **3a–3i** и **5a–5i** без катализатора

Table 1

***In vitro* antibacterial and antifungal activity of compounds 3a-3i and 5a-5i**
***Таблица 1. In vitro* антибактериальная и противогрибковая активность соединений 3a-3i и 5a-5i**

Compounds №	Growth inhibition zones, mm		
	Candida albicans	Gram-positive bacteria ***S.aureus***	Gram-negative **E.coli**
3a	-	-	-
3b	-	-	-
3c	-	-	14
3d	-	-	

Continuation of the Table 1

3e	-	-	16
3f	-	-	-
3g	-	-	-
3h	-	12	13
3i	-	15	15
5a	16	25	28
5b	-	-	-
5c	-	-	-
5d	10	16	18
5e		13	15
5f		-	-
5g	22	29	30
5h	21	30	30
5i	-	-	-
Furadonine		25	24
Furazolidone		25	24
Fluconazole 50 mg/ml	25		
Fluconazole 150 mg/ml	33		

EXPERIMENTAL SECTION

Compounds **3a-3i** and **5a-5i** were prepared as previously reported [25, 26].

Antibacterial and antifungal activity.

All used chemicals had analytical grade. The synthesized compounds were screened *in vitro* for their antibacterial activity against two strains of bactria, *S. aureus*, *E. coli*, and antifungal activity against *C. albicans* strain, by the agar diffusion method [29]. The inoculum was applied Sabouraud (for fungi) and nutrient agar (for pathogenic bacteria). From bacterial and fungal biomass in sterile saline solution, suspensions were prepared, where 1 ml suspension of *E. coli* contains $2 \cdot 10^8$ bacteria, and 1 ml suspension of *S. aureus* contains $2.5 \cdot 10^8$ bacteria. 1 ml suspension of *C. albicans* contains $1 \cdot 10^8$ fungal cells. The hospital strains of pathogenic microorganisms were taken from the Department of Epidemiology of Yerevan State Medical University after M. Heratsi. Solutions of the synthesized compounds were poured (0.2 mL) into cylinders placed on the surface of an agar medium inoculated with test strain in Petri dishes, and by a spatula it was evenly distributed over the surface of the nutrient agar and sabouraud agar. After all, were made wells (with a diameter of 8 mm) and the test substances (dissolving 50 mg of substance in 1 mL of solvent DMSO was done) were collected in 0.1 mL to these wells (0.1 mL of DMSO solvent contains 5 mg of the synthesized substances). After 20 h of culture at 37 °C, the diameters of growth inhibition zones were measured. The tests were repeated three times. The zones of inhibition were measured in millimetre to estimate the potency of the tested compounds. The synthetic agents with systemic antimicrobial action, Furazolidone and Furadonine (50 mg were taken as a control) (manufactured by JSC Borisov Plant of Medical Preparations, Republic of Belarus) and both doses of 50 mg and 150 mg of Fluconazole were taken as a control, (synthesized and patented by Pfizer (USA) were used as positive controls. Dimethylformamide (DMFA) was also used as a solvent, the results showed no significant difference/data.

Molecular docking study

In order to have insights into the better activity of compounds, we did molecular docking studies. Molecular docking studies were conducted to evaluate the binding affinities and molecular interactions of potential compounds, aiming to uncover the structure-based mechanisms that drive their *in vitro* antimicrobial activity. By simulating interactions between the compounds and key microbial targets, these studies offer insights into how the compounds bind to active sites and impact the biological processes of bacterial and fungal pathogens, aiding in the optimization for improved antimicrobial efficacy.

Docking simulation were performed by using AutoDock VINA integrated in the PyRx 0.8 [31] virtual screening tool to identify compounds with high binding affinity. *Insilico* docking simulation studies to evaluate the molecular interactions of **5a, 5d, 5g,** and **5h** compounds were done with the *E. coli,* Flavoprotein (NfsA) (PDB:7NB9) [32] with a co-crystallised antagonist Nitrofurantoin (U6Z) with a resolution of 1.09 Å and C. *albicans*, Sterol 14-alpha demethylase (CYP51) (PDB: 5TZ1) in complex with anti-fungal

ligand VT1161 (VT1) or *Oteseconazole* with a resolution of 2.00 Å [33].

The selection of antibacterial and antifungal targets was driven by their demonstrated *in vitro* activity and relevance to the compounds under investigation. *E. coli* NfsA was chosen as an antibacterial target due to the structural similarity of the compounds to Nitrofurantoin, a well-known antimicrobial agent. This similarity suggests that the compounds may interact with the NfsA protein in a comparable manner, potentially leading to effective inhibition of the bacterial enzyme. For the antifungal targets, *C. albicans* CYP51 was selected because it represents a broad-spectrum antifungal target critical for fungal cell membrane synthesis. The compounds were evaluated against *C. albicans* in *in vitro* antimicrobial assays. These rational targets were selected to uncover the underlying mechanisms of antimicrobial activity against both bacterial and fungal pathogens, with the aim of assessing their potential for broad-spectrum efficacy. Protein structures were processed to ensure an optimized structure for docking studies and it was executed with UCSF Chimera Dock Prep module and that includes the following steps: elimination of water molecules and other ligands, addition of missing atoms and residues, energy minimization and assigning Gasteiger partial charges and polar hydrogens and then converted to the pdbqt format.

Molecular interaction summary of compounds with *E. coli* NfsA

The 2D structure of the ligands was drawn with ChemDraw software and the structures were optimized through energy minimization with MMFF94 force field parameters and optimization was done with conjugate gradient algorithm in Open Babel module of PyRx and then eventually converted the ligands to the AutoDock compatible pdbqt format to carry out docking exploration.

Autodock Vina grid box was created around the antagonist active site with the following details of the vina search space: **7NB9**: Centre (***Å)*** X: 4.839, Y: -22.809, Z: -6.791, **5ZT1**: X: 71.372 , Y: 66.694, Z: 4.726, with Dimensions (***Å)*** X: 25.00, Y: 25.00, Z: 25.00, Spacing (***Å***) = 0.375.

Post docking analysis and visualization of binding poses and molecular interactions were done with BIOVIA Discovery Studio 2021 and Chimera X tools [34]. The validation procedure for the docking program meticulously involved the re-docking of VT-1161 into its co-crystallized site. The remarkably low Root Mean Square Deviation (RMSD) value of 1.95 Å, observed between the docked (white) and native poses (grey), strongly indicates the program's effectiveness in precisely predicting the binding pose of VT-1161. The binding energies and molecular interaction profiles of the compounds will be compared to those of Nitrofurantoin and VT-1161. These co-crystallized antagonist ligands are well-established antimicrobial drugs effective against bacterial and fungal targets.

Table 2

Binding affinity outcomes obtained from the Molecular interaction summary of docking asessments compounds with *E.coli* NfsA

Таблица 2.* Результаты связывания, полученные из сводки молекулярных взаимодействий соединений, содержащих NfsA *E.coli

Compounds	Binding Energy (K.cal/mol)	Interacting Amino acids	Nature of interactions
5a	-6.6	SER41, SER40, SER39, PHE42, SER38, ASP107, LEU103, GLU99	H-bond, alkyl, van der waals
5d	-6.2	SER41, SER40, SER39, PHE42, SER38, ASP107, MET110	H-bond, π- π stacked, van der waals
5g	-5.9	SER39, SER38, PHE42, SER41, SER40, GLN44, ARG35, THR37, ALA36	H-bond, π- π T-shaped, π-alkyl, carbon hydrogen bond, van der waals
5h	-7.1	SER41, SER40, SER39, PHE42, SER38, THR37	H-bond, π- π stacked, π-alkyl, carbon hydrogen bond, van der waals

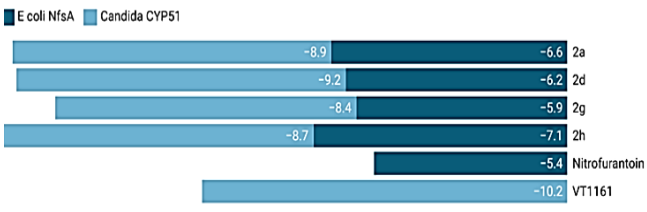

Fig. 1. Binding energy plot of compounds with E. coli NfsA and *Candida* CYP51

Рис. 1. График энергии связывания соединений с E. coli NfsA и *Candida* CYP51

Molecular interaction profile of compounds with *E.coli* NfsA

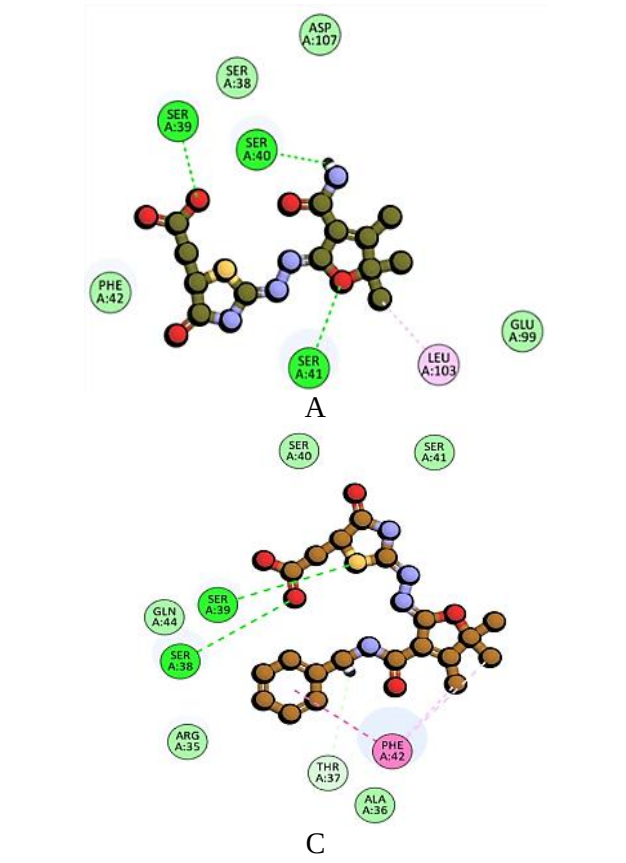

Fig. 2. 2D molecular representation of interactions of compounds A) **5a**, B) **5d**, C) **5g**, D) **5h**, with the active site residues of the *E.coli* NfsA protein. Interactions were displayed as color coded dashed lines, green lines indicated the H–bonds

Рис. 2. Двумерное молекулярное изображение взаимодействий соединений A) **5a**, B) **5d**, C) **5g**, D) **5h** с остатками активного центра белка NfsA *E. coli*. Взаимодействия обозначены цветными пунктирными линиями, зелёные линии обозначают водородные связи

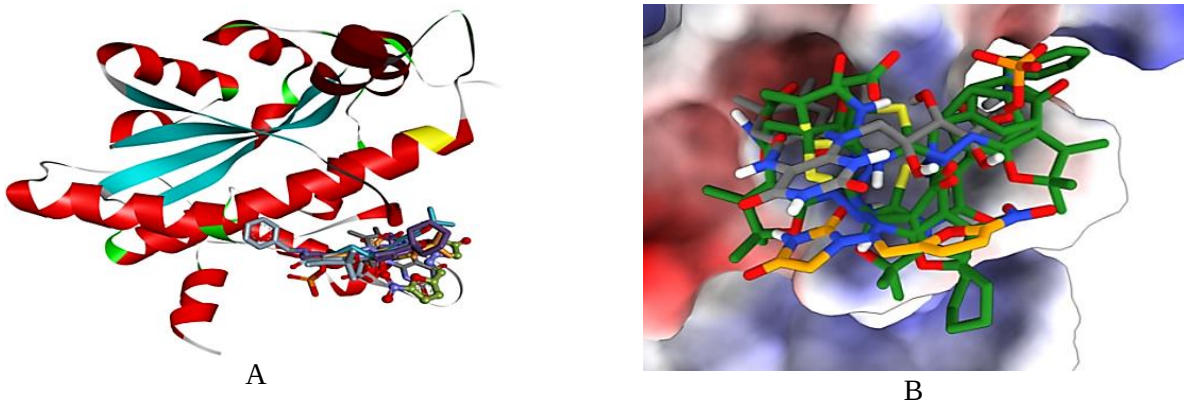

Fig. 3. Protein ligand complexes (A) representing the binding modes of **5a**, **5d**, **5g**, **5h** compounds and Nitrofurantoin (gold with ball and stick filled representtation) (B) *E.coli* NfsA protein surface representing the compounds (green with stick representation) and Nitrofurantoin (Yellow with stick representation) and FMN (grey with stick representation) in the active site pocket

Рис. 3. Комплексы белковых лигандов (A), представляющие способы связывания соединений **5a**, **5d**, **5g**, **5h** и нитрофурантоина (золотой с заполненными шариками и палочками) (B) Поверхность белка *E. coli* NfsA, представляющая соединения (зеленый с палочками), а также нитрофурантоин (желтый с палочками) и ФМН (серый с палочками) в кармане активного центра

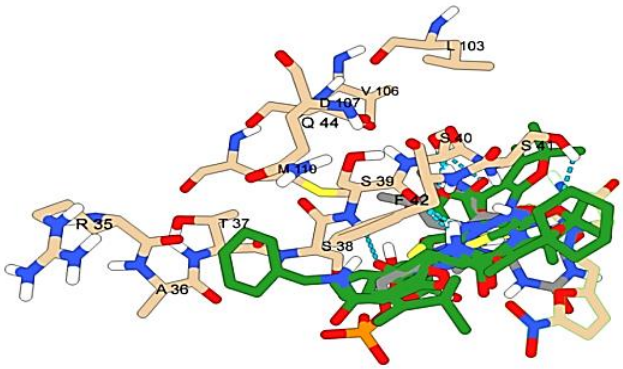

Fig. 4. Molecular alignment representing the binding modesand active site residues displaying common hydrogen bonding interactions of **5a**, **5d**, **5g** and **5h** compounds green with stick representation) and Nitrofurantoin and FMN (Orange and grey with ball and stick representation)

Рис. 4. Молекулярное выравнивание, представляющее способы связывания, и остатки активного центра, демонстрирующие общие взаимодействия водородных связей соединений **5a**, **5d**, **5g** и **5h** (зеленый с представлением палочки) и нитрофурантоина и ФМН (оранжевый и серый с представлением шарика и палочки)

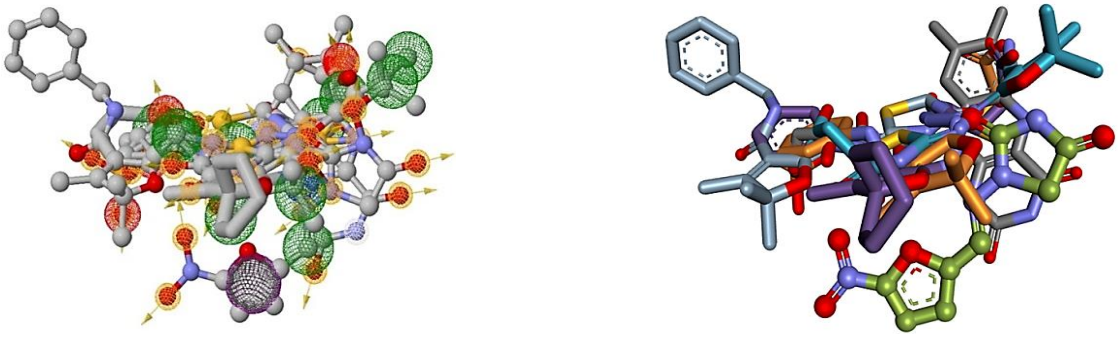

A B

Fig. 5. A) Molecular alignment of the binding poses and B) Pharmacophore features of compounds **5a**, **5d**, **5g** and **5h** and Nitrofurantoin (gold color with ball and stick representation). The pharmacophore feature color coding is as follows: purple spheres: aromatic groups, green spheres: hydrophobic groups, orange spheres: hydrogen bond donors (HBD), and white spheres: hydrogen bond acceptors (HBA)

Рис. 5. A) Молекулярное выравнивание позиций связывания и B) Фармакофорные характеристики соединений **5a**, **5d**, **5g** и **5h** и нитрофурантоина (золотой цвет с обозначением в виде шарика и палочки). Цветовая кодировка фармакофорных характеристик следующая: фиолетовые сферы: ароматические группы, зелёные сферы: гидрофобные группы, оранжевые сферы: доноры водородных связей (HBD), белые сферы: акцепторы водородных связей (HBA)

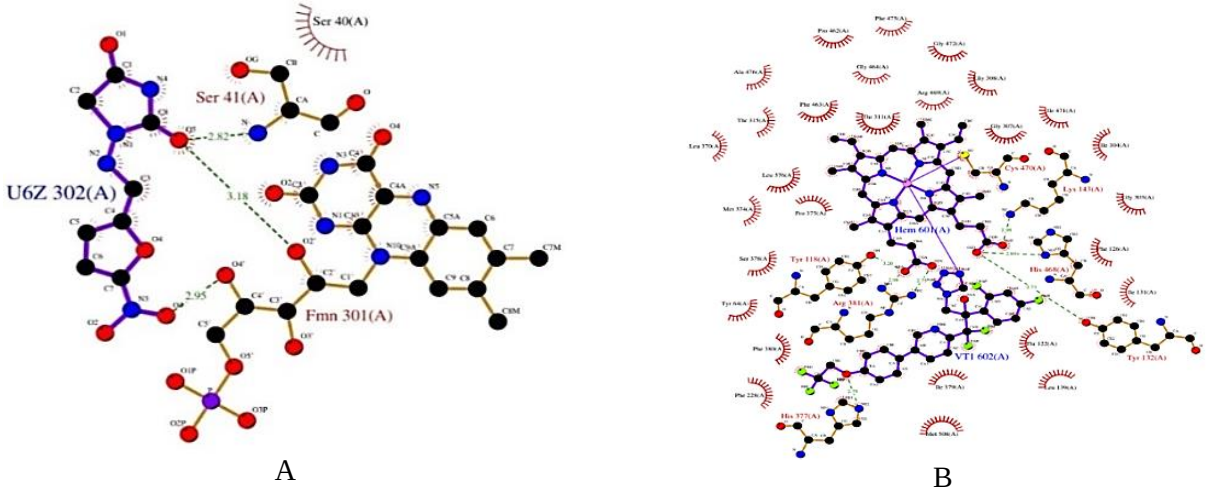

A B

Fig. 6. A) LigPlot interactions of Nitrofurantoin (U6Z) and FMN, B) VT1161 (VT1) and HEM displaying thecritical hydrogen bond interactions that includes SER41 with *E.coli* NfsA and TYR118, TYR132, LYS143, HIS377, ARG381, HIS468 with *Candida albicans* CYP51

Рис. 6. A) Взаимодействия LigPlot нитрофурантоина (U6Z) и FMN, B) VT1161 (VT1) и HEM, демонстрирующие критические взаимодействия водородных связей, включающие SER41 с *E. coli* NfsA и TYR118, TYR132, LYS143, HIS377, ARG381, HIS468 с *Candida albicans* CYP51

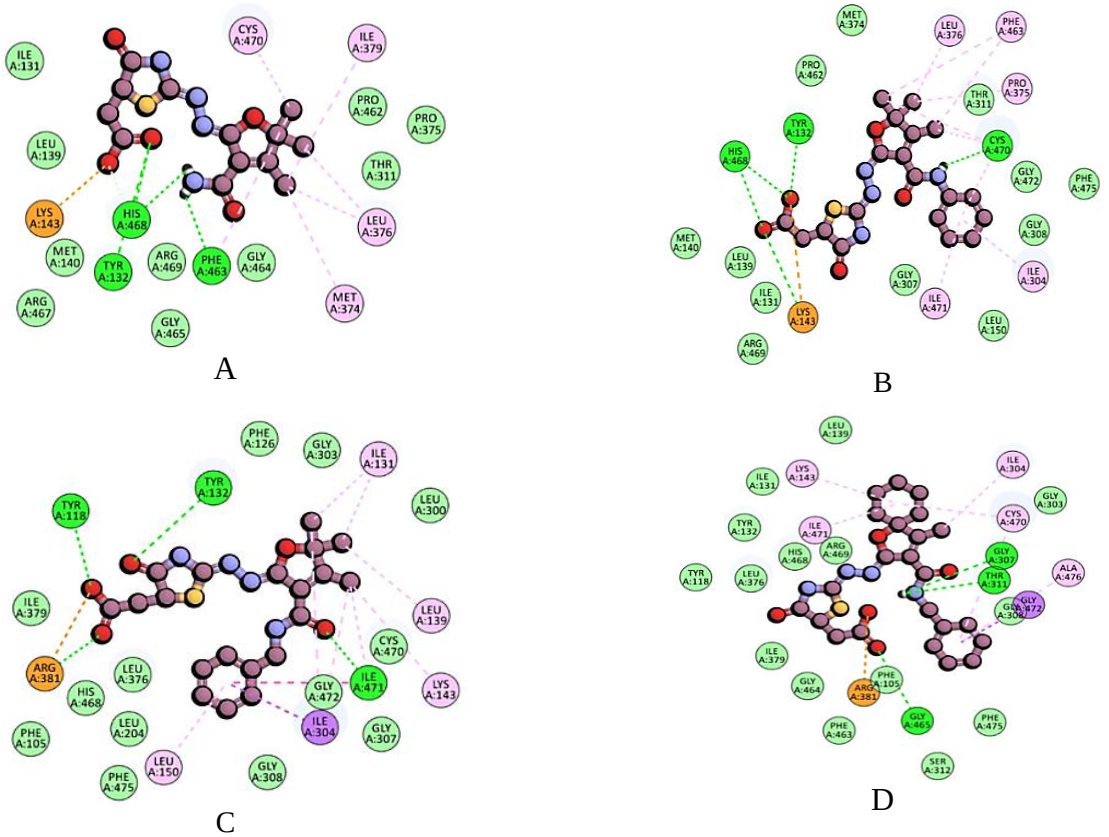

Fig. 7. 2D molecular representation of interactions of compounds A) **5a**, B) **5d**, C) **5g**, D) **5h**, with the active site residues of the *C. albicans*, CYP51protein. Interactions were displayed as color coded dashed lines, green lines indicated the H–bonds

Рис. 7. Двумерное молекулярное изображение взаимодействий соединений A) **5a**, B) **5d**, C) **5g**, D) **5h** с остатками активного центра белка CYP51 *C. albicans*. Взаимодействия отображены цветными пунктирными линиями, зелёные линии обозначают водородные связи

Table 3

Molecular interaction summary of compounds with *Candida* CYP51

***Таблица 3*. Сводка молекулярного взаимодействия соединений с *Candida* CYP51**

Compounds	Binding Energy (K.cal/mol)	Interacting Amino acids	Nature of interactions
5a	-8.9	HIS468, TYR132, PHE463, LYS143, MET374, LEU376, ILE379, CYS470, ILE131, LEU139, MET140, ARG467, ARG469, GLY465, GLY464, PRO462, PRO375, THR311	H-bond, π-alkyl, alkyl, carbon hydrogen bond, salt bridge, van der waals
5d	-9.2	HIS468, TYR132, CYS470, LYS143, ILE471, ILE304, PRO375, PHE463, LEU376, MET374, PRO462, MET140, LEU139, ILE131, ARG469, GLY307, LEU150, GLY308, GLY472, PHE475, THR311	H-bond, π-alkyl, alkyl, carbon hydrogen bond, attractive charge, van der waals
5g	-8.4	TYR132, TYR118, ILE471, ARG381, ILE304, ILE131, LEU139, LYS143, LEU150, PHE126, GLY303, LEU300, CYS470, GLY472, GLY307, GLY308, ILE379, LEU376, HIS468, PHE105, LEU204, PHE475	H-bond, π-alkyl, π-sigma, alkyl, amide-π stacked, salt bridge, van der waals
5h	-8.7	THR311, GLY307, GLY465, ARG381, GLY472, ALA476, CYS470, ILE304, LYS143, ILE471, LEU139, ILE131, TYR132, TYR118, LEU376, HIS468, ARG469, ILE379, GLY464, PHE105, PHE463, PHE475, SER312, GLY308, GLY303	H-bond, π-alkyl, π-sigma, alkyl, salt bridge, van der waals

Molecular interaction profile of compounds with *C. albicans* CYP51

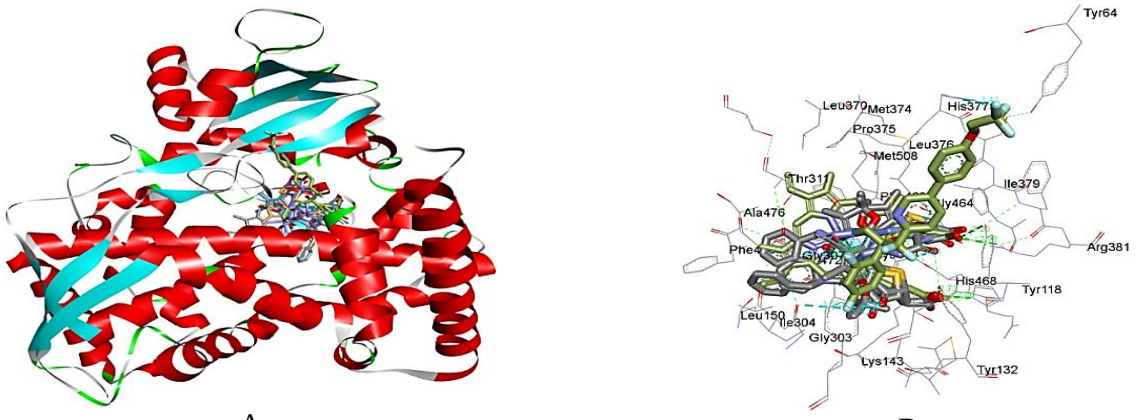

A B

Fig. 8. Protein ligand complexes (A) representing the binding modes of **5a**, **5d**, **5g**, **5h** compounds HEM and VT1 (gold with stick representation) (B) Molecular alignment representing the binding modesof **5a**, **5d**, **5g**, **5h** compounds and VT1 displaying common hydrogen bonding interactions with active site residues HIS468 and TYR132

Рис. 8. Комплексы белковых лигандов (A), представляющие способы связывания соединений **5a**, **5d**, **5g**, **5h** HEM и VT1 (золото с изображением палочки) (B) Молекулярное выравнивание, представляющее способы связывания соединений **5a**, **5d**, **5g**, **5h** и VT1, демонстрирующее общие взаимодействия водородных связей с остатками активного центра HIS468 и TYR132

Molecular interaction profile analysis of compounds with *E. coli* NfsA

Docking simulations on the *E. coli* NfsA protein revealed that compound **5h** (3-benzylcarbamoyl 1-oxaspiro) exhibited the strongest binding energy of -7.1 kcal/mol, followed closely by **5a** (3-carbamoyl) and **5d** (3-phenylcarbamoyl) with binding energies of -6.6 and -6.2 kcal/mol, respectively. These compounds displayed notable similarities in their interaction profiles. Compound **5g** (3-benzylcarbamoyl) showed slightly weaker binding energy at -5.9 kcal/mol. Overall, all compounds demonstrated superior binding energy and interaction profiles compared to Nitrofurantoin (-5.4 kcal/mol). The enhanced binding affinities suggest that these compounds form favorable interactions with the target protein, potentially contributing significantly to their biological activity.

The compound **5a** exhibited three hydrogen bond interactions with consecutive serine residues in the active site: SER39, SER40, and SER41. The carbamoyl group and the oxygen atom of the furan ring formed hydrogen bonds with SER40 and SER41, respectively, while the acetic acid moiety on the 4-oxo-thiazolidine ring established a hydrogen bond with SER39. These serine residues are critical for interactions with FMN (SER39) and Nitrofurantoin (SER41). Additionally, one of the methyl groups of the dimethyl substituent on the furan ring displayed an alkyl hydrophobic interaction with the LEU103 residue. Other key binding site residues, including SER38, ASP107, PHE42, and GLU99, contributed through van der Waals interactions.

Compound **5d** displayed a hydrogen bond interaction profile similar to that of compound **5a**, involving the same key active site residues, including SER39, SER40, and SER41. These interactions were complemented by an additional π-π stacking interaction with the PHE42 residue, mediated by the phenyl group attached to the carbamoyl moiety. Additionally, compound **5d** formed van der Waals interactions with residues ASP107, MET110, and SER38, further contributing to its binding stability within the active site.

Compound **5g** exhibited two hydrogen bond interactions: one with SER38 via the carbonyl group of the acetic acid moiety and another with SER39 through the sulfur atom of the 4-oxo-thiazolidine ring. PHE42 engaged in a T-shaped π-π interaction with the benzyl aromatic ring and π-alkyl interactions with the methyl groups of the furan ring. Additionally, THR37 established a carbon-hydrogen bond with the benzyl ring, while van der Waals interactions were observed with residues SER40, SER41, GLN44, ARG35, and ALA36 within the active site.

Compound **5h** demonstrates hydrogen bond interactions with a triad of serine residues (SER39, SER40, and SER41), similar to compounds **5a** and **5d**. Specifically, SER39 forms hydrogen bonds with the nitrogen atoms of the 4-oxo-thiazolidine ring and the carbamoyl group, while SER40 interacts with the carboxylic group of the acetic acid substituent on the same ring. SER41 engages with the hydrazone linker connecting the heterocyclic rings. Additionally, SER42 participates in π-π stacking with the benzyl aromatic ring and π-alkyl interactions with the methyl group of

the oxospiro ring. SER38 establishes carbon-hydrogen bond interactions with the 4-oxo group of the thiazolidine ring and van der Waals interactions with THR37.

Flavin Mononucleotide (FMN), the native substrate of the flavin protein, interacts with the active site in the presence of Nitrofurantoin. SER39 forms a hydrogen bond with one of the hydroxyl groups on the linker and participates in amide-π stacking interactions with the dihydrobenzopteridine ring. MET110 and VAL106 exhibit alkyl interactions with the dimethyl groups on the benzene ring in the central scaffold, while SER40 establishes π-donor hydrogen bond interactions with the same ring. Additionally, SER38, PHE42, and ASP107 engage in van der Waals interactions. Notably, Nitrofurantoin, positioned close to FMN, forms a critical hydrogen bond with SER41.

Compounds **5a, 5d**, and **5h**, which display similar critical hydrogen bond interactions with SER41 (Fig. 6A) and comparable structural features, also engage with SER39 in hydrogen bonding interactions akin to FMN. This mirroring of interactions likely contributes to their potential antibacterial activity against *E. coli*. The binding pocket orientations (Fig. 3B) reveal that compounds **5a, 5d, 5g**, and **5h** occupy the active site in a manner similar to Nitrofurantoin, which engages in limited interactions primarily with SER41. These compounds, however, demonstrate a broader range of interactions, enhancing their stabilization and binding affinities. Additionally, molecular alignment and pharmacophore analysis (Fig. 5A and 5B) indicate a significant overlap in pharmacophore features with Nitrofurantoin.

The interaction analysis is depicted in 2D interaction diagrams (Fig. 2), highlighting the various interactions between the compounds and the active site residues of the target protein. Figure 6 focuses on the interactions of Nitrofurantoin, while Fig. 4 presents a 3D representation of the molecular alignment and binding poses of the compounds alongside Nitrofurantoin, emphasizing hydrogen bonds with key binding site residues. Additionally, Fig. 3A and 3B illustrate the binding modes of the compounds within the active site and the pocket surface.

Molecular interaction profile analysis of compounds with *Candida albicans* CYP51.

Docking simulations performed on the *C. albicans* protein indicate that compounds **5d** (-9.2 K.cal/mol) exhibited better binding affinity and interaction profiles compared to other compounds.

VT1, a co-crystallized antifungal drug, primarily interacts with the HEM porphyrin's Feion and HIS377. These interactions play a crucial role in its binding and activity. Most of the compounds evaluated in this docking simulation demonstrated strong interactions with key HEM-binding residues, such as TYR118, TYR132, PHE463 and HIS468. The interaction profile of HEM and VT1 is depicted in Fig. 5B.

These compounds showed binding energies and interaction profiles comparable to VT1 (-10.2 kcal/mol). With their strong *in-silico* performance in docking simulations, these hit compounds hold promising potential and warrant further investigation and optimization for development as effective antifungal agents.

Compound **5a** formed three hydrogen bonds with TYR132, HIS468, and PHE463, facilitated by the acetic acid moiety and the carbamoyl group. A salt bridge interaction was observed between LYS143 and the carboxylic group of the acetic acid linked to the thiazolidine ring. Hydrophobic alkyl interactions were identified between the methyl groups of the furan ring and residues CYS470, ILE379, LEU376, and MET374. Additionally, HIS468 displayed a carbon-hydrogen bond interaction, while the remaining binding site residues participated in van der Waals interactions.

Compound **5d** displayed a comparable interaction pattern to **2a,** forming hydrogen bonds with TYR132 and HIS468. A key distinction was observed in the carbamoyl interaction: **5d** interacted with CYS470, whereas **5a** engaged with PHE463. Additionally, LYS143 contributed through attractive charged interactions. Additionally, π-alkyl interactions with ILE304 and ILE471 were mediated by the phenyl group linked to the carbamoyl moiety. The compound's methyl groups also formed alkyl interactions with CYS470, PRO375, PHE463, and LEU376 residues.

Compound **5g** exhibited four hydrogen bond interactions with active site residues TYR132, TYR118, ARG381, and ILE471, mediated by the 4-oxo and acetic acid moieties on the thiazolidine ring, as well as the carbamoyl linker. The benzyl ring formed π-sigma interactions with ILE304 and amide-π stacked interactions with ILE471. ARG381 also engaged in a salt bridge interaction with the acetic acid moiety. The trimethyl substituents on the furan ring formed alkyl interactions with ILE131, LEU139, LYS143, and ILE304, while LEU150 demonstrated π-alkyl interactions with the benzyl ring.

Compound **5h** demonstrated a distinct hydrogen bonding profile compared to **5a** and **5d,** forming interactions with GLY307, THR311, and GLY465, primarily mediated by the acetic acid and carbamoyl groups. A salt bridge interaction was observed between ARG381 and the acetic acid moiety. Additionally, GLY472 exhibited π-sigma interactions, while ALA476 and CYS470 formed π-alkyl interactions with the ben-

zyl ring. The spiro ring participated in alkyl interactions with ILE304, LYS143, and ILE471, complemented by van der Waals interactions with adjacent residues in the binding site.

The molecular interaction profile of the **5a**, compounds with CYP51 is illustrated in Fig. 6, while the respective binding site orientations and critical hydrogen bond interactions are depicted in Fig. 8 (A and B).

In all compounds, the terminal acetic acid moiety and the carbamoyl group play a critical role in forming hydrogen bonds and hydrophobic interactions with key residues.

However, the hydrazo linker connecting the furan and thiazole rings does not contribute to any significant interactions. This lack of contribution is attributed to the internalization of the hydrazo linker when the compounds adopt stable binding conformations. Consequently, the carbamoyl and acetic acid groups are exposed, facilitating their interactions with the critical residues.

Determination of ADMET and Druglikness Profile.

ADMET properties (absorption, distribution, metabolism, excretion, and toxicity) are crucial in drug development for successful progression to clinical trials. To evaluate the pharmacokinetic properties of our compounds, we performed an *in-silico* assessment using pkCSM webserver https://biosig.lab.uq.edu.au/pkcsm/prediction [35].

Table 4

ADMET properties of potential compounds with pkCSM

Таблица 4. **ADMET-свойства потенциальных соединений с pkCSM**

Compounds	Absorption			Distribution		Metabolism		Excretion		Toxicity				
	Water solubility Log mol/L	Human Intestinal Absorption (%)	Caco2 permeability log Papp in 10^{-6} cm/s	VDss (log L/kg)	BBB Permeability (log BB)	CYP450 isoform Inhibitors	CYP450 isoform Substrates	Total Clearance (ml/min/kg)	Renal OCT2 substrate	Max. tolerated dose (Log mg/kg/day)	Skin Sensitization	Hepatotoxicity	AMES toxicity	hERG I and II inhibiton
5a	-3.268	47.862	0.866	-1.194	-1.066	-	3A4	-0.142	No	0.774	No	Yes	No	No
5d	-3.628	47.862	0.866	-1.194	-1.066	-	3A4	-0.142	No	0.774	No	Yes	No	No
5g	-3.482	45.401	0.634	-1.261	-1.002	-	3A4	-0.123	No	0.683	No	Yes	No	No
5h	-3.795	52.119	0.625	-1.058	-1.034	-	3A4	-0.197	No	0.514	No	Yes	No	No

Toxicity assessments reveal no concerns for AMES toxicity, skin sensitization, or hERG I and II inhibition, suggesting that the compounds do not exhibit significant mutagenic or cardiac toxicity risks. However, all compounds show hepatotoxicity, which warrants further investigation in terms of liver safety and potential mitigation strategies.

CONCLUSION

We have developed the catalyst-free and eco-friendly synthesis of compounds **3a-i** and **5a-i** comprising iminodihydrofuran and thiazolidinone rings by subsequent Michael addition/heterocyclization reaction from iminodihydrofuran thiosemicarbazones. To attach a thiazolidinone scaffold to iminodihydrofuran a thiourea linker was used. The methodologies are simple, efficient and inexpensive affording good to excellent yields of the polyheteroconjugated products with operational simplicity.

Compounds **5a, 5d, 5g, 5h** have pronounced antimicrobial activity against 3 pathogenic microorganisms. Compounds **5a, 5g, 5h** showed higher antibacterial activity against the bacteria *S. aureus* and *E. coli* than the standard drugs Furadonin and Furazolidone. Compounds **5g, 5h** showed very good antifungal activity against the fungus *C. albicans*. The results indicated that the tested organisms experienced a noticeable inhibition of fungal and bacterial growth.The ADMET profiles indicate that these compounds, particularly **5h** with the highest human intestinal absorption, possess favorable characteristics for further optimization and development. Although they exhibit hepatotoxicity, refining their pharmacokinetic properties is essential for advancing these hit compounds as potential antimicrobial agents.

CONFLICT OF INTEREST

The authors declare the absence a conflict of interest warranting disclosure in this article.

Авторы заявляют об отсутствии конфликта интересов, требующего раскрытия в данной статье.

REFERENCES
ЛИТЕРАТУРА

1. **Abdul-Rida N.A., Mohammed K.T.** New biaryl derivatives of diclofenac drug: synthesis, molecular docking and their biological activity study as anticancer and antioxidant agents. *ChemChemTech [Izv. Vyssh. Uchebn. Zaved. Khim. Khim. Tekhnol.]*. 2024. V. 67. N 12. P. 47-53. DOI: 10.6060/ivkkt.20246712.7071.
Абдул-Рида Н.А., Мохаммед К.Т. Новые биарильные производные препарата диклофенака: синтез, молекулярный докинг и изучение их биологической активности как противораковых и антиоксидантных средств. *Изв. вузов. Химия и хим. технология.* 2024. Т. 67. Вып. 12. С. 47-53.
2. **Lyadov V.A., Makrushin D.E., Denislamova E.S., Maslivets A.N., Triandafilova G.A., Solodnikov S.I.** Synthesis and analgesic activity of methyl-1-antipyryl-4-aroyl-2,3-dioxo-2,3,5,10-tetrahydrobenzo[b]pyrrolo[2,3-e][1,4]diazepine-10a(1H)-carboxylates. *ChemChemTech [Izv. Vyssh. Uchebn. Zaved. Khim. Khim. Tekhnol.]*. 2024. V. 67. N 5. P. 17-23 (in Russian). DOI: 10.6060/ivkkt.20246705.6939.
Лядов В.А., Макрушин Д.Е., Денисламова Е.С., Масливец А.Н., Триандафилова Г.А., Солодников С.Ю. Синтез и анальгетическая активность метил-1-антипирил-4-ароил-2,3-диоксо-2,3,5,10-тетрагидробензо[b]пирроло[2,3-e][1,4]диазепин-10a(1H)-карбоксилатов. *Изв. вузов. Химия и хим. технология.* 2024. Т. 67. Вып. 5. С. 17-23.
3. **Khazimullina Yu.Z., Gimadieva A.R.** Synthesis and antiradical activity of conjugates of uracil derivatives with amino acids. *ChemChemTech [Izv. Vyssh. Uchebn. Zaved. Khim. Khim. Tekhnol.]*. 2023. V. 66. N 2. P. 36-44 (in Russian). DOI: 10.6060/ivkkt.20236602.6652.
Хазимуллина Ю.З., Гимадиева А.Р. Синтез и антирадикальная активность конъюгатов производных урацила с аминокислотами. *Изв. вузов. Химия и хим. технология.* 2023. Т. 66. Вып. 2. С. 36-44.
4. **Deng J.C.** Viral–bacterial interactions–therapeutic implications. *Influenza Other Respir. Viruses.* 2013. V. 7. P. 24-35. DOI: 10.1111/irv.12174.
5. **Pfaller M. A., Diekema D.J.** Epidemiology of Invasive Candidiasis: A Persistent Public Health Problem. *Clin. Microbiol. Rev.* 2007. V. 20. P. 133–163. DOI: 10.1128/CMR.00029-06.
6. WHO fungal priority pathogens list to guide research, development and public health action. Geneva, Switzerland. 2022.
7. **Godzishevskaya A.A., Lopashinova E.P., Kurasova M.N., Kritchenkov A.S., Andreeva O.I.** Mechanical, antibacterial and antiproliferative properties of iridium- and rhodium-containing chitosan films. *ChemChemTech [Izv. Vyssh. Uchebn. Zaved. Khim. Khim. Tekhnol.]*. 2023. V. 66. N 8. P. 92-98. DOI: 10.6060/ivkkt.20236608.6782.
Годзишевская А.А., Лопашинова Е.П., Курасова М.Н., Критченков А.С., Андреева О.И. Механические, антибактериальные и антипролиферативные свойства иридий- и родийсодержащих хитозановых пленок. *Изв. вузов. Химия и хим. технология.* 2023. Т. 66. Вып. 8. С. 92-98.
8. **Tripathi C., Gupta S.J., Fatima G.N., Sonar P.K., Verma A., Saraf S.K.** 4-Thiazolidinones: The advances continue *Eur. J. Med. Chem.* 2014. V. 72. P. 52–77. DOI: 10.1016/j.ejmech.2013.11.017.
9. **Mishchenko M., Shtrygol S., Kaminskyy D., Lesyk R.** Thiazole-bearing 4-thiazolidinones as new anticonvulsant agents. *Sci. Pharm.* 2020. V. 88. N 1. P. 16-30. DOI: 10.3390/scipharm88010016.
10. **Nazeef M., Neha K., Ali S., Ansari K., Danish M., Tiwari S.K., Yadav V., Siddiqui I.R.** Visible-light-promoted C–N and C–S bonds formation: A catalyst and solvent-free photochemical approach for the synthesis of 1,3-thiazolidin-4-ones. *J. Photochem. Photobiol. A: Chem.* 2020. V. 390. P. 112347-112354. DOI: 10.1016/j.jphotochem.2019.112347.
11. **Popiołek Ł., Piątkowska-Chmiel I., Gawro´nska-Grzywacz M., Biernasiuk A., Izdebska M., Herbet M., Sysa M., Malm A., Dudka J., Wujec M.** New hydrazide-hydrazones and 1,3-thiazolidin-4-ones with 3-hydroxy-2-naphthoic moiety: Synthesis, in vitro and in vivo studies. *Biomed. Pharmacother.* 2018, V. 103. P. 1337–1347. DOI: 10.1016/j.bmc.2016.04.06.
12. **Pejovi´c A., Mini´c A., Jovanovi´c J., Pe˘si´c M., Komatina D.I., Damljanovi´c I., Stevanovi´c D., Mihailovi´c V., Katani´c J., Bogdanovi´c G.A.** Synthesis, characterization, antioxidant and antimicrobial activity of novel 5-arylidene-2-ferrocenyl-1,3-thiazolidin-4-ones. *J. Organomet. Chem.* 2018. V. 869. P. 1–10. DOI: 10.1016/j.jorganchem.2018.05.014.
13. **Agrawal N.** Synthetic and therapeutic potential of 4-thiazolidinone and its analogs. *Curr. Chem. Lett.* 2021. V. 10. P. 119–138. DOI: 10.5267/j.ccl.2020.11.002.
14. **Avetisyan A.A., Tokmadjyan G.G.** Biologically active derivatives of 2-butene and 3-butene-4-olides. *Chem. J. Arm.* 1993. V. 46. N 3–4. P. 219–236 (in Russian).
Аветисян А.А., Токмаджян Г.Г. Биологически активные производные 2-бутен и 3-бутен-4-олидов. *Хим. Ж. Армении.* 1993. Т. 46. № 3–4. С. 219–236.
15. **Avetisyan A.A., Tokmadjyan G.G.** Achievement of chemistry of 2-butene 4-olides. *Chem. J. Arm.* 2007. V. 60. N 4. P. 698–712 (in Russian). **Аветисян А.А., Токмаджян Г.Г.** Успехи химии 2-бутен-4-олидов. *Хим. Ж. Армении*. 2020. Т. 60. № 4. С. 698–712. DOI: 10.46991/PYSU:B/2020.54.1.012.
16. **Tokmajyan G.G., Karapetyan L.V., Paronikyan R.V., Stepanyan H.M.** Synthesis and antibacterial activity of new derivatives of 2-oxo-2,5-dihydrofu¬rans containing an oxothiazolidinylidene ring. *Proc. Yerevan State Univ. (Chem. Biol.)*. 2020. V. 54. N 1. P. 12–16.
17. **Husain, A.; Khan, Sh.A.; Iqbal, M.A.; Asif, M.** Insights into the chemistry and therapeutic potential of furanones: A versatile pharmacophore. *Eur. J. Med. Chem.* 2019. V. 171. P. 66-92. DOI: 10.1016/j.ejmech.2019.03.021.
18. **Villamizar-Mogotocoro A.-F., Leon-Rojas A.F., Urbina-Gonzalez J.M.** Δα,β-Butenolides [Furan-2(5H)-ones]: Ring Construction Approaches and Biological Aspects - A Mini-Review. *Mini-Rev. Org. Chem.* 2020. V. 17. N 8. P. 922-945. DOI: 10.2174/1570193X17666200220130735.
19. **Badovskaya L.A., Poskonin V.V., Tyukhteneva Z.I.** 2(5H)-Furanone and 5-Hydroxy-2(5H)-furanone: Reactions and Syntheses Based on Them. *Russ. J. Gen. Chem.* 2021. V. 91. N 2. P. 133-153. DOI: 10.1134/S1070363221020018.
20. **Fan H., Wei X., Si-Tu M.-X., Lei Y.-H., Zhou F.-G., Zhang C.-X.** γ-Aromatic Butenolides of Microbial Source – A Review of Their Structures, Biological Activities and Biosynthesis. *Chem. Biodiversity*. 2022. V. 19. N 6. P. e202200208. DOI: 10.1002/cbdv.202200208.
21. **Avetisyan A.A., Karapetyan L.V., Paronikyan R.V., Stepanyan G.M.** Synthesis and antibacterial activity of new 2.5-dihydrofuran derivatives. *Pharm. Chem. J.* 2011. V. 45. N 3. P. 156–158. DOI: 10.1007/s11094-011-0582-2.

22. **Avetisyan A.A., Karapetyan L.V., Paronikyan R.V., Stepanyan G.M.** Synthesis and antibacterial activity of 4-(2-R-vinyl) derivatives of functionally substituted 2,5-dihydrofurans. *Pharm. Chem. J.* 2011. V. 45. N 12. P. 723–724. DOI: 10.1007/s11094-012-0711-6.
23. **Tokmajyan G., Karapetyan L., Paronikyan R., Stepanyan H.** Synthesis and antibacterial activity studies of new 2-N-substituted-2,5-dihydrofuran-3-carboxamides. *Pol. Sci. J.* 2018. V. 7. P. 7–11.
24. **Tokmajyan G.G., Karapetyan L.V., Paronikyan R.V., Stepanyan H.M.** Synthesis and antibacterial activity studies of new 2-N-substituted-2,5-dihydrofuran-3-carboxamides. *Proc. Yerevan State Univ. (Chem. Biol.).* 2019. V. 53. N 3. P. 156–160.
25. **Karapetyan L.V., Tokmajyan G.G.** Catalyst-Free Synthesis of New Iminodihydrofurans Containing Thiazolidinone Ring. *Chemistry Select*. 2022. V. 7. N 44. P. e20220274. DOI: 10.1002/slct.202202745.
26. **Karapetyan L.V., Tokmajyan G.G.** Synthesis of New Derivatives of 2-Imino-2,5-dihydrofurans Containing 4-Oxothiazolidine Ring. *Russ. J. Gen. Chem.* 2023. V. 93. N 3. P. 506-512. DOI: 10.1134/S1070363223030076.
27. **Karapetyan L.V., Tokmajyan G.G., Makaryan G.M.** Synthesis of Novel 2-(N-Substituted)imino-2,5-dihydrofuran-3-carboxamides Containing a Thiourea Residue and an Oxothiazolidinylidene Ring. *Russ. J. Org. Chem.* 2019. V. 55. N 11. P. 1806–1808. DOI: 10.1134/S1070428019110265.
28. **Karapetyan L.V., Tokmajyan G.G., Paronikyan R.V.** Synthesis and Antibacterial Activity of New Polyheteroconjugated and Dinuclear Systems Based on N-Substituted 2-Imino-2,5-dihydrofuran-3-carboxamides. *Russ. J. Org. Chem.* 2021. V. 57. N 1. P. 131–134. DOI: 10.1134/S1070428021010206.
29. Guidelines for conducting preclinical studies of medicinal products. Pt. 1. Ed. by A.N. Mironov. M.: I-vo Grif i K. 2012. P. 109-254 (in Russian). Руководство по проведению доклинических исследований лекарственных средств. Ч. 1. Под ред. А.Н. Миронова. М.: Гриф и К. 2012. С. 109-254.
30. **Mashkovsky M.D.** Medicines. M.: Novaya Volna. 2020. 1216 p. (in Russian). **Машковский М.Д.** Лекарственные средства. М.: Новая волна. 2020. 1216 с.
31. **Dallakyan S., Olson A.J.** Small-Molecule Library Screening by Docking with PyRx. In: Chemical Biology. Methods in Molecular Biology. Ed. by J. Hempel, C. Williams, C. Hong. 2015. V. 1263. NY.: Humana Press. DOI: 10.1007/978-1-4939-2269-7_19.
32. **Day M.A., Jarrom D., Christofferson A.J., Graziano A.E., Anderson J.L.R, Searle P.F., Hyde E.I. , White S. A.** The structures of E. coli NfsA bound to the antibiotic nitrofurantoin; to 1,4-benzoquinone and to FMN. *Biochem. J.* 2021. V. 478. N 13. P. 2601-2617. DOI: 10.1042/BCJ20210160.
33. **Hargrove T.Y., Friggeri L., Wawrzak Z., Qi A., Hoekstra W.J., Schotzinger R.J., York J.D., Guengerich F.P., Lepesheva G.I.** Structural analyses of Candida albicans sterol 14-demethylase complexed with azole drugs address the molecular basis of azole-mediated inhibition of fungal sterol biosynthesis. *J. Biol. Chem.* 2017. V. 292. N 16. P. 6728-6743. DOI: 10.1074/jbc.M117.778308.
34. **Pettersen E.F., Goddard T.D., Huang C.C., Meng E.C., Couch G.S., Croll T.I., Morris J.H., Ferrin T.E.** UCSF ChimeraX: Structure visualization for researchers, educators, and developers. *Protein Sci.* 2021. V. 30. N 1. P. 70-82. DOI: 10.1002/pro.3943.
35. **Pires D.E.V., Blundell T.L., Ascher D.B.** pkCSM: Predicting Small-Molecule Pharmacokinetic and Toxicity Properties Using Graph-Based Signatures. *J. Med. Chem.* 2015. V. 58. N 9. P. 4066–4072. DOI: 10.1021/acs.jmedchem.5b00104.

Поступила в редакцию 12.05.2025
Принята к опубликованию 15.10.2025

Received 12.05.2025
Accepted 15.10.2025